



Ultrathin atomic layer deposited ZrO₂ coating to enhance the electrochemical performance of Li₄Ti₅O₁₂ as an anode material

Jian Liu^a, Xifei Li^a, Mei Cai^b, Ruying Li^a, Xueliang Sun^{a,*}

^a Department of Mechanical and Materials Engineering, University of Western Ontario, London, ON, Canada N6A 5B9

^b General Motors R&D Center, Warren, MI 48090-9055, USA

ARTICLE INFO

Article history:

Received 27 November 2012

Received in revised form

23 December 2012

Accepted 28 December 2012

Available online 26 January 2013

Keywords:

Zirconium oxide

Atomic layer deposition

Lithium-ion battery

Lithium titanate

ABSTRACT

Atomic layer deposition (ALD) was used to deposit ZrO₂ directly on Li₄Ti₅O₁₂ electrode to improve its electrochemical performance. The thickness of the deposited ZrO₂ was controlled by adjusting ALD cycles from 0 to 1, 2, 5, 10 and 50. The Li₄Ti₅O₁₂ electrodes with and without ZrO₂ coating were characterized by scanning electron microscope, energy dispersive X-ray spectroscopy, high-resolution transmission electron microscope, cyclic voltammetry (CV) and galvanostatic charge-discharge test. The CV result indicated that ZrO₂ coating with 2, 5 and 10 ALD cycles could effectively reduce the electrochemical polarization of the Li₄Ti₅O₁₂ electrode. Charge-discharge test revealed that the Li₄Ti₅O₁₂ electrodes with 1-, 2- and 5-cycle ZrO₂ coating exhibited higher specific capacity, better cycling performance and rate capability than the pristine Li₄Ti₅O₁₂ in a voltage range of 0.1–2.5 V. However, ZrO₂ coating with more than 5 ALD cycles could lead to degraded performance of Li₄Ti₅O₁₂. Mechanism for the enhanced electrochemical performance of Li₄Ti₅O₁₂ was explored by electrochemical impedance spectroscopy, and the reason was attributed to the suppressed formation of solid electrolyte interphase and the improved electron transport by ultrathin ZrO₂ coating.

© 2013 Elsevier Ltd. All rights reserved.

1. Introduction

Recently, considerable efforts have been made to developing high performance Li-ion batteries (LIBs) in the applications of power electric vehicles (EVs) and plug-in hybrid electric vehicles (PHEVs) [1,2]. As the electrochemical performance of LIBs strongly depends on the electrode materials, it is of great importance to select proper anode and cathode materials. At present, graphite is widely used in commercial LIBs as the anode material, but it suffers from poor abuse tolerance for EV and PHEV applications [3]. Spinel Li₄Ti₅O₁₂ (LTO) has attracted increasing attention as an alternative to graphite due to its high working potential of the redox couple Ti⁴⁺/Ti³⁺ (*ca.* 1.55 V vs. Li/Li⁺) [4]. One advantage of LTO over other anode materials is the negligible volume change during charge/discharge process, because of which LTO is known as a “zero-strain” material [5,6]. Besides the structural stability, LTO is also found to exhibit good thermodynamic stability due to its compatibility with electrolyte, promising LIBs a good safety for EV and PHEV applications [7]. However, LTO exhibits an inherently insulating property owing to the empty Ti 3d-sates with band gap energy of ~2 eV, which seriously hinders its high-rate performance [6,8]. To solve this problem, two strategies are

generally adopted, *i.e.* reducing the physical diffusion length of electrons and Li-ions by preparing nanosized LTO materials [9–14], or/and enhancing the Li-ion diffusion and electronic conductivity *via* surface modification or ion doping [9,10,15–18]. By means of these methods, the drawback of LTO has been overcome to a great extent, and its high rate performance has been improved greatly [9–18]. Currently, LTO has been considered as one of the most promising anode materials in practical energy applications [19].

In most previous studies, the electrochemical performance of LTO was evaluated in a voltage window of higher than 1 V, because the redox couple Ti⁴⁺/Ti³⁺ operates at 1.55 V (vs. Li/Li⁺) [4]. Recently, there is increasing awareness that it is necessary to study the LIB performance of LTO at a lower voltage than 1 V, in view of the following aspects: (1) It is important to study the over-charge behaviors of LTO for safety concern, as uneven electrodes will result in local polarization and local overcharge during lithium uptake process [20,21]; (2) LTO electrodes operate at a lower voltage could offer a higher discharge capacity and a higher cell voltage, thereby resulting in higher energy density of LIBs [22–26]. It was widely reported that the discharge capacity of LTO could exceed its theoretical capacity of 175 mAh g⁻¹ (based on Li₄Ti₅O₁₂/Li₇Ti₅O₁₂ transition), when the voltage window extended down to 0 V [22–26]. For example, LTO powders prepared by a solid state method exhibited a discharge capacity of 155 mAh g⁻¹ after 50 cycles between 1

* Corresponding author. Tel.: +1 519 661 2111x87759; fax: +1 519 661 3020.

E-mail address: xsun@eng.uwo.ca (X. Sun).

and 2 V, while a higher specific capacity of 190 mAh g^{-1} after 50 cycles could be achieved in a voltage range of 0.1–2 V [24]. The extra discharge capacity resulted from the further reduction of Ti^{4+} between 0.6 and 0.1 V, which was repeatable in the subsequent cycles [22–27]. However, the increased capacity of LTO by extended voltage window was accompanied by the decomposition of electrolyte between 0.5 and 1 V, which would lead to the formation of solid electrolyte interphase (SEI) [21]. Therefore, suppressing the formation of SEI becomes important in order to enhance the cycling performance and coulombic efficiency of LTO in an extended voltage window [28,29].

Recently, atomic layer deposition (ALD) technique has attracted increasing attention in the field of LIBs [30,31], for its capability to realize excellent coverage and conformal deposition of thin films with precisely controlled thickness at nanoscale level [32]. As to the application in anodes, ALD- Al_2O_3 is the most studied coating material, and Al_2O_3 coating has been found to be able to alleviate the cracking of the anodes during charge-discharge process [33,34], suppress the side reactions between anodes and electrolyte [33–36], mitigate the decomposition of SEI, especially at elevated temperatures [34,37], and preserving mechanical integrity of the electrodes by “knitting” the active materials to the conductive additive [37,38], thereby improving the LIB performance. Besides Al_2O_3 , ZrO_2 is another excellent coating material for both anodes [39] and cathodes [40,41] in LIBs. To our best knowledge, ALD coating of ZrO_2 has not been demonstrated in the application of LIB anodes so far. In the present work, therefore, we use ALD- ZrO_2 coating to modify the LTO electrode in order to improve its LIB performance in an extended voltage window (0.1–2.5 V). The effect of ZrO_2 coating with different thicknesses on the LIB performance of the LTO electrode was investigated in details, and it was demonstrated that only ZrO_2 coating with no more than 5 ALD cycles can enhance the electrochemical performance of the LTO. Underlying mechanism for the improvement was explored and discussed.

2. Experimental

2.1. Material preparation and characterization

Nanoflower-like LTO powders were synthesized by a microwave assisted hydrothermal method and following heat treatment, and the detailed process was described in our previous work [42]. To prepare the electrode, the LTO powders, acetylene black and polyvinylidene fluoride binder (PVDF), with a weight ratio of 80:10:10, were mixed homogeneously, and then the slurry was pasted onto a copper foil. The obtained electrode was dried under vacuum at 110 °C for 12 h. ALD- ZrO_2 was achieved using tetrakis(dimethylamido)zirconium (IV) ($\text{Zr}(\text{NMe}_2)_4$) and water as precursors at a deposition temperature of 100 °C. Detailed procedure of ALD- ZrO_2 was reported in our previous study [43]. Coating of ALD- ZrO_2 was conducted directly on the as-prepared LTO electrode, with different ALD cycles (0, 1, 2, 5, 10 and 50). In the following section, the LTO electrode coated with 0, 1, 2, 5, 10 and 50-cycle ZrO_2 is referred as LTO-0, LTO-1, LTO-2, LTO-5, LTO-10 and LTO-50, respectively. The loading of active materials (including ZrO_2 if applicable) is ~2.23, 2.32, 2.39, 2.41, 2.46 and 2.71 mg for LTO-0, LTO-1, LTO-2, LTO-5, LTO-10 and LTO-50, respectively.

The morphology and structure of the above samples were characterized by a field-emission scanning electron microscope (SEM, Hitachi S4800) equipped with energy dispersive X-ray spectroscopy (EDS) and high-resolution transmission electron microscope (HRTEM, JEOL 2010 FEG).

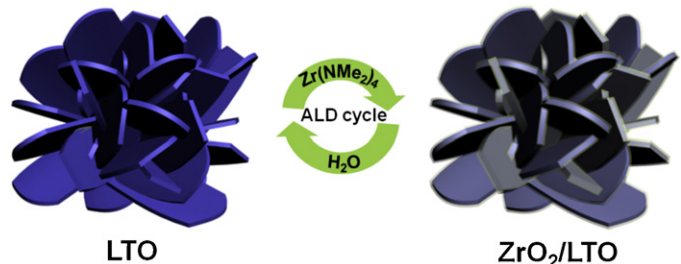


Fig. 1. Schematic diagram of LTO and LTO coated with ZrO_2 by ALD.

2.2. Electrochemical characterization

Electrochemical measurements were performed by using coin-type half cells assembled in an argon-filled glove box ($[\text{O}_2] < 1 \text{ ppm}$, $[\text{H}_2\text{O}] < 1 \text{ ppm}$). The coin-type half-cell consisted of the LTO electrodes prepared above, polypropylene separator (Celgard 2400), and lithium foil as the counter electrode. The electrolyte was 1 M LiPF_6 solution in ethylene carbonate (EC): diethyl carbonate (DEC): ethyl methyl carbonate (EMC) with a volume ratio of 1:1:1. The electrochemical performance of the coin-type half cells was tested in an Arbit BT-2000 Battery Test System.

3. Results and discussion

It was reported that ZrO_2 could be deposited by ALD using $\text{Zr}(\text{NMe}_2)_4$ and H_2O as precursors in a wide temperature range of 50–300 °C [43,44]. In this work, the same precursor combination was adopted for ALD- ZrO_2 , which was directly applied on the LTO electrode at 100 °C. Typically the first ALD- ZrO_2 reaction requires a hydroxyl-terminated surface, which is present on metal oxides [35]. According to published work [43,44], each ALD cycle should deposit a uniform ZrO_2 layer of approximately 0.096–0.142 nm in thickness. After different ALD cycles, the surface of LTO was covered by uniform ZrO_2 film, as schematically shown in Fig. 1.

Fig. 2 displays the morphologies of the LTO electrodes with and without ZrO_2 coating. The initial LTO consists of many nanosheets with wall thickness of ~18 nm, as seen in Fig. 2a. For LTO-1 and LTO-2, there is no visible change in the morphology, as indicated in Fig. 2(b and c). For LTO-5, the edges of nanosheets are lighter than the central parts, which might be induced by the ZrO_2 coating, as presented in Fig. 2d. In Fig. 2e, it is obvious that LTO-10 has thicker nanosheets and slightly rougher surface than LTO-0, due to the ZrO_2 coating. 50-cycle ALD leads to the growth of ZrO_2 film on the surface of nanosheets, the thickness of which is measured to be ~35 nm for LTO-50. The higher growth per cycle of ZrO_2 in this case is due to the large surface area of nanoflower-like LTO ($46.8 \text{ m}^2 \text{ g}^{-1}$) [42], which makes completely purge of H_2O from reactor difficult. During the pulse of $\text{Zr}(\text{NMe}_2)_4$, the presence of H_2O in the reactor leads to slightly enhanced growth per cycle resulting from some chemical vapor deposition. SEM images of the above samples at low magnification are included in Fig. SI-1. EDS analysis confirms the existence of Zr and O elements in the ALD- ZrO_2 coated samples, and the intensity of Zr element increases with ALD cycles (Fig. SI-2). Furthermore, the EDS mapping reveals the uniform distribution of Zr and O elements on the LTO, and Fig. 3 shows the EDS mapping result of LTO-10 as an example.

To further study the ZrO_2 coating on the LTO, HRTEM was performed on LTO-10, and the result is showed in Fig. 4. The lattice distance of LTO-10 is measured to be 0.485 nm, in agreement well with $d_{(111)}$ spacing of spinel $\text{Li}_4\text{Ti}_5\text{O}_{12}$ (JCPDS PDF No. 49-0270). In Fig. 4, it is evident that the surface of LTO-10 is covered by a dense and uniform thin film, as marked by the red dash lines. EDS of HRTEM further verifies the presence of Zr and O elements

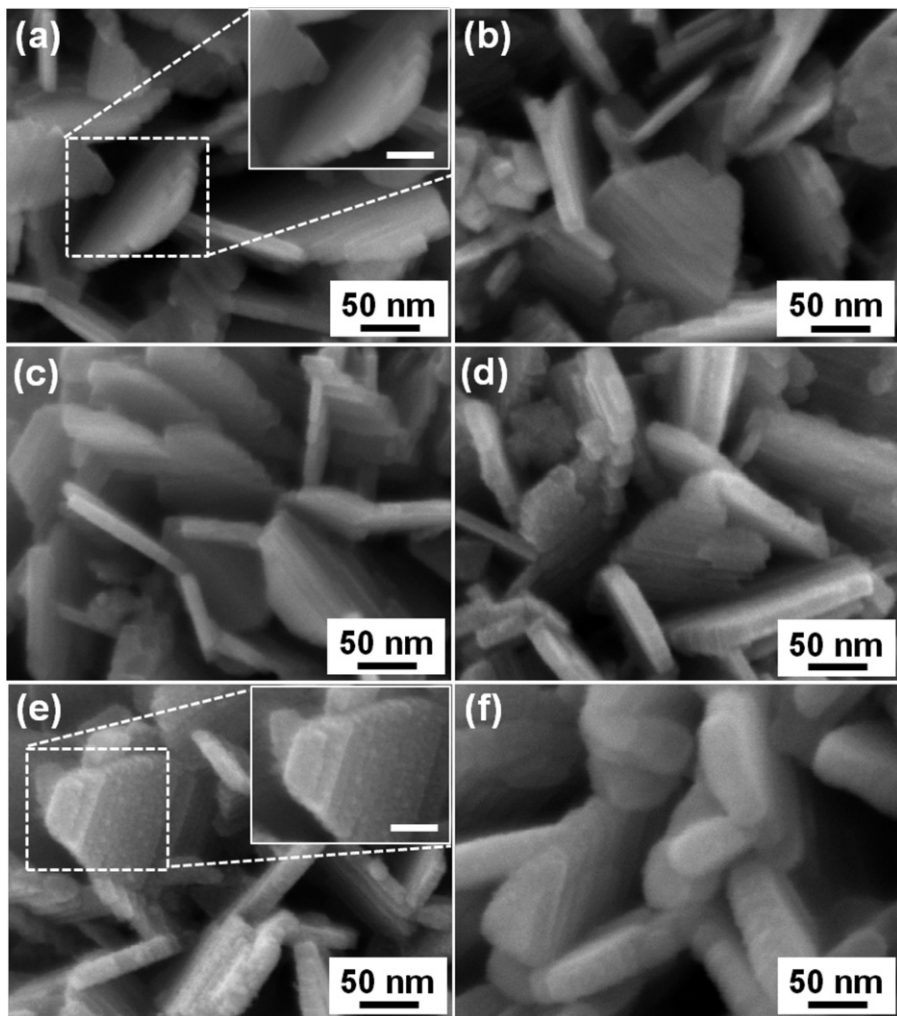


Fig. 2. SEM images of (a) LTO-0, (b) LTO-1, (c) LTO-2, (d) LTO-5, (e) LTO-10 and (f) LTO-50 (the scale bars in the insets of Fig. 1a and e represent 30 nm).

in LTO-10. The ZrO_2 coating layer is determined to be ~ 2 nm in thickness. Based on the results of SEM, EDS and HRTEM, it can be concluded that uniform ZrO_2 films with different thicknesses were successfully coated on the LTO electrode by ALD.

The electrochemical performance of the LTO electrodes with and without ZrO_2 coating was evaluated in order to study the ZrO_2 coating effect systematically. Fig. 5 shows the cyclic voltammograms (CVs) of different samples in the first three cycles. In Fig. 5, one can see that between 1 and 2.5 V, one pair of redox peaks appears at about 1.70 V (anodic) and 1.47 V (cathodic) for all the samples, which are correlated to the spinel/rock-salt phase transition ($\text{Li}_4\text{Ti}_5\text{O}_{12}/\text{Li}_7\text{Ti}_5\text{O}_{12}$) [12–15]. It is obvious that even at such a low scanning rate (0.1 mV s^{-1}), the degree of the electrochemical polarization is different among the samples. Table 1 compares the potential differences between the anodic and cathodic peaks in the

first five cycles (anodic and cathodic peak potentials are included in SI-Table 1). It can be found that the potential difference gradually decreases with ZrO_2 coating up to 10 ALD cycles, and then experiences an increase with 50-cycle ZrO_2 coating. For example, the potential difference in the fifth cycle is 0.315, 0.281, 0.171, 0.178, 0.178 and 0.321 V for LTO-0, LTO-1, LTO-2, LTO-5, LTO-10 and LTO-50, respectively. The narrowed potential differences of LTO-2, LTO-5 and LTO-10 indicate the reduced polarization and enhanced electrochemical kinetics of the LTO electrodes by ZrO_2 coating with no more than 10 ALD cycles. Insets of Fig. 5 show the enlarged CVs below 1 V, and one can find another couple of reduction and oxidation peaks located between 0.1 and 0.6 V. Those two peaks are observed to be repeatable in the subsequent cycles, and therefore enlarging the potential window can increase the reversible capacity of the LTO electrode. The reduction peak below 0.6 V could be attributed to the further reduction of Ti^{4+} [27]. When $\text{Li}_4\text{Ti}_5\text{O}_{12}$ is charged to $\text{Li}_7\text{Ti}_5\text{O}_{12}$, only one Ti^{4+} is reduced and there are still $2/3 \text{ Ti}^{4+}$ remaining in the reduction production of $\text{Li}_7\text{Ti}_5\text{O}_{12}$ to accept electrons [27,45]. Further intercalation of lithium ions into $\text{Li}_7\text{Ti}_5\text{O}_{12}$ below 0.6 V could occupy the tetrahedral (8a) sites, leading to the increased reversible capacity of spinel $\text{Li}_4\text{Ti}_5\text{O}_{12}$ [45].

Fig. 6 displays the charge/discharge profiles of the LTO electrodes with and without ZrO_2 coating during the first two cycles. It can be seen that all the samples except LTO-50 exhibit flat plateaus near 1.55 V and inclined curves between 0.1 and 0.6 V (vs. Li/Li^+), which agree well with the two pairs of redox peaks in the CVs

Table 1

Potential differences (V) between anodic peak and cathodic peaks in the first five cycles.

	1st cycle	2nd cycle	3rd cycle	4th cycle	5th cycle
LTO-0	0.398	0.243	0.213	0.250	0.315
LTO-1	0.297	0.247	0.253	0.268	0.281
LTO-2	0.196	0.167	0.165	0.152	0.171
LTO-5	0.197	0.176	0.176	0.175	0.178
LTO-10	0.201	0.184	0.175	0.184	0.178
LTO-50	0.289	0.268	0.264	0.271	0.321

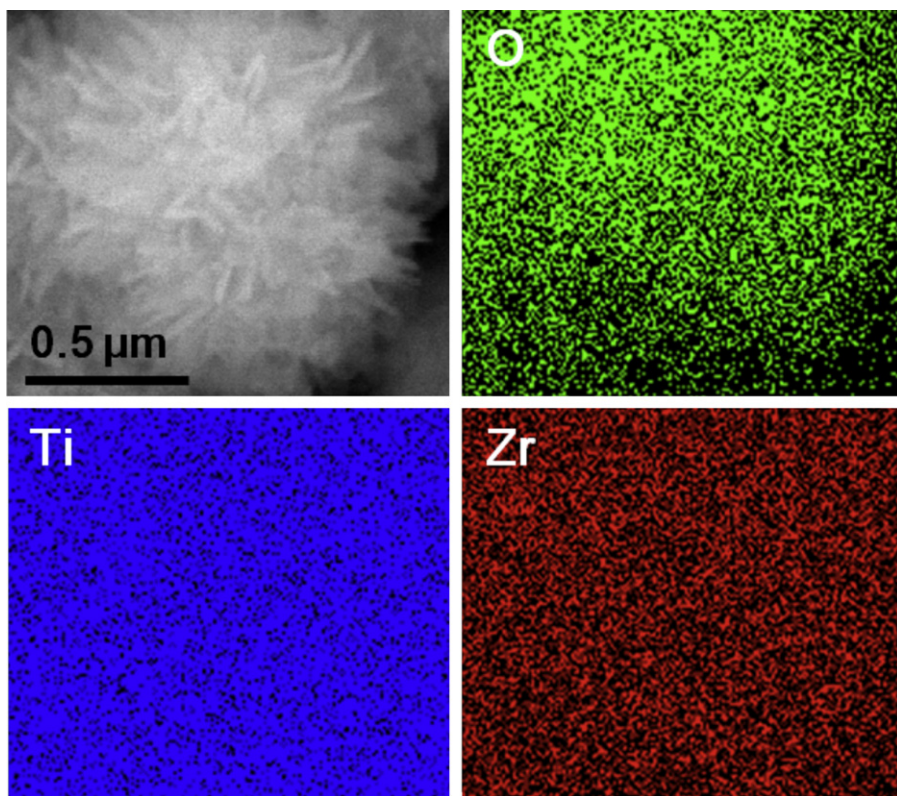


Fig. 3. EDS mapping of LTO-10.

(Fig. 5). LTO-50 shows continuously decreased potential with the intercalation of lithium ions in the LTO during the first cycle, which is probably due to the inhibited lithium ion diffusion by thick insulating ZrO_2 layer. In Fig. 6, it is apparent that the discharge/charge capacities of LTO-0 are lower than those of LTO-1, LTO-2, LTO-5 and LTO-10, but higher than LTO-50. For example, the discharge capacity in the second cycle is 216, 226, 230, 224, 222 and 180 mAh g^{-1} for LTO-0, LTO-1, LTO-2, LTO-5, LTO-10 and LTO-50, respectively. This result suggests that appropriate ZrO_2 coating can improve the discharge/charge capacities of the LTO. For all the samples, there are obvious capacity losses after the first cycle, which could be attributed to the SEI formation below 1 V [28,29].

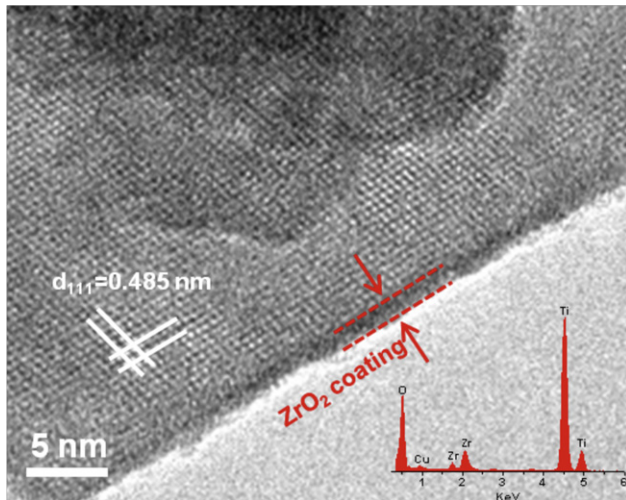


Fig. 4. HRTEM image of LTO-10 (inset shows the EDS result).

Fig. 7 presents the cycling stabilities and rate capabilities of the LTO electrodes with and without ZrO_2 coating between 0.1 and 2.5 V. The cycling stabilities in Fig. 7a indicates that LTO-1, LTO-2, LTO-5 and LTO-10 exhibit higher specific capacity and better cycling performance than LTO-0 and LTO-50 at a current density of 200 mA g^{-1} . The initial discharge capacity is 310, 330, 343, 350, 343 and 216 mAh g^{-1} for LTO-0, LTO-1, LTO-2, LTO-5, LTO-10 and LTO-50, respectively. All the samples show obvious capacity losses in the second cycle, due to the irreversible lithium ions trapped in the SEI [28,29]. Then the irreversible capacity rapidly decreases upon cycling, and the reversible capacity stabilizes after ca. 20 cycles.

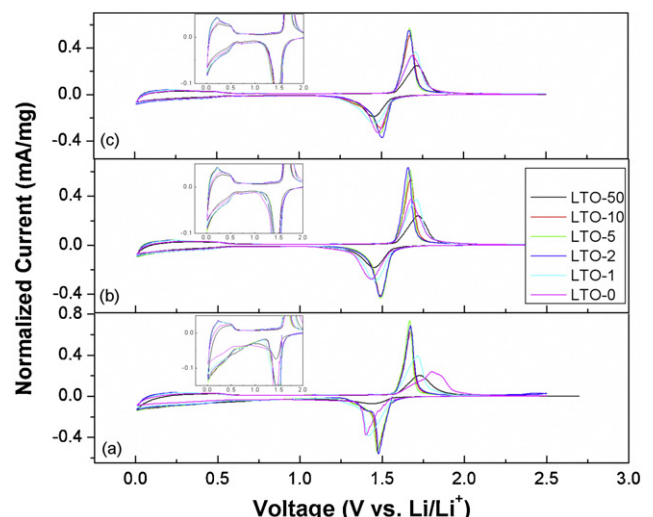


Fig. 5. CV curves of LTO-0, LTO-1, LTO-2, LTO-5, LTO-10 and LTO-50 during the (a) first, (b) second and (c) third cycle at a scanning rate of 0.1 mV s^{-1} between 0.1 and 2.5 V (insets show the enlarged parts below 1 V).

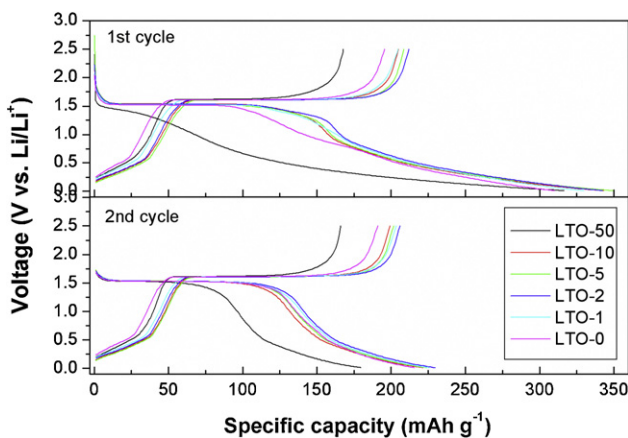


Fig. 6. Charge/discharge profiles of LTO-0, LTO-1, LTO-2, LTO-5, LTO-10 and LTO-50 in the first and second cycles between 0.1 and 2.5 V at a current density of 200 mA g^{-1} .

After 100 cycles, LTO-0, LTO-1, LTO-2, LTO-5, LTO-10 and LTO-50 can maintain a specific capacity of 152, 169, 168, 168, 166 and 148 mA g^{-1} , respectively. The coulombic efficiency (CE) of each sample is compared in Fig. 7b. The CE in the first cycle is determined to be 63%, 62%, 62%, 60%, 60% and 53% for LTO-0, LTO-1, LTO-2, LTO-5, LTO-10 and LTO-50, respectively. In the following cycles, the CE increases greatly for all the samples, and keeps at $\sim 100\%$ after 20 cycles. In the inset of Fig. 7b, one can easily find that LTO-50 has much higher CE than the others after the first cycle, suggesting that ZrO_2 coating can effectively suppress further decomposition of electrolyte and the formation of SEI after the first cycle. Fig. 7c presents the rate capabilities of all the samples at various current

densities (50 – 1600 mA g^{-1}), and the second-cycle discharge capacity at each current density is compared in Fig. 7d. In Fig. 7c, it can be found that the rate capabilities of LTO-1, LTO-2 and LTO-5 are obviously better than that of LTO-0, especially at a high current density of 1600 mA g^{-1} , while LTO-50 shows worse rate capability than LTO-0. The rate capability of LTO-10 is comparable with that of LTO-0. With the increase of the current density, the discharge capacity gradually decreases for all the samples, as seen in Fig. 7d. At a current density of 1600 mA g^{-1} , the discharge capacity is 90, 103, 101, 106, 86 and 41 mAh g^{-1} for LTO-0, LTO-1, LTO-2, LTO-5, LTO-10 and LTO-50, respectively. Moreover, all the samples can recover the initial reversible capacity at 50 mA g^{-1} . Based on the CV and charge-discharge tests, it can be concluded that ZrO_2 coating with no more than 5 ALD cycles can improve the specific capacity, cycling performance and rate capability of the LTO electrode.

To find out the reason for the improved electrochemical performance, electrochemical impedance spectroscopy (EIS) measurement of the LTO electrodes with and without ZrO_2 coating was carried out at about 1.5 V in a frequency range from 0.1 to 10^4 Hz , and typical Nyquist plots are given in Fig. 8. It can be seen the Nyquist plots of LTO-0, LTO-2, LTO-5, LTO-10 and LTO-50 are composed of two partially overlapped and depressed semicircles in the high-frequency and middle-frequency ranges, and one inclined line at low frequency (except LTO-50). The EIS curves are simulated using the equivalent circuit in the inset of Fig. 8, and one can find that the experimental and simulated data are almost coincident. Accordingly, the depressed semicircles at high frequency can be attributed to the resistance of SEI film (R_{sei}), those at middle frequency are caused by charge-transfer resistance (R_{ct}) at the interface of electrolyte and electrode, and the sloped lines at low frequency can be considered to be the Warburg impedance (W) [25,28,29]. R_s is the solution resistance, and CPE1 and CPE2 are

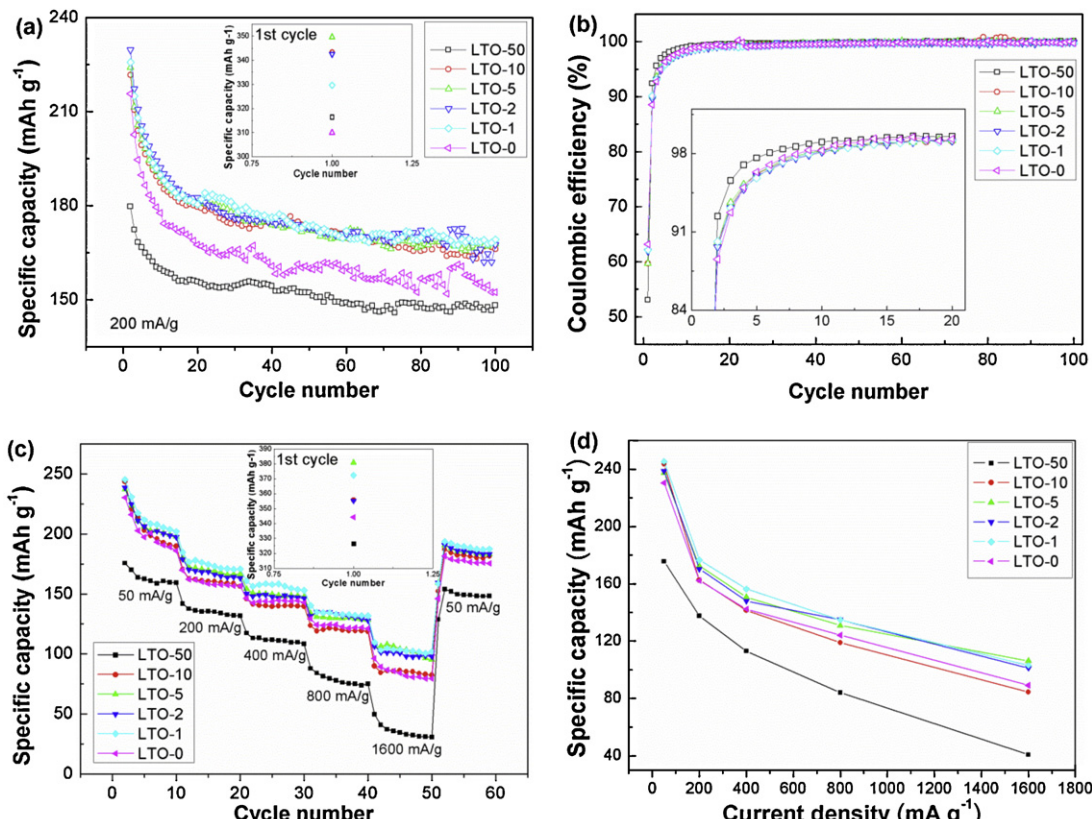


Fig. 7. (a) Cycling stability, (b) coulombic efficiency, (c) rate capability and (d) discharge capacity vs. current density of LTO-0, LTO-1, LTO-2, LTO-5, LTO-10 and LTO-50 between 0.1 and 2.5 V (insets in Fig. 6a and c show the discharge capacity in the first cycle).

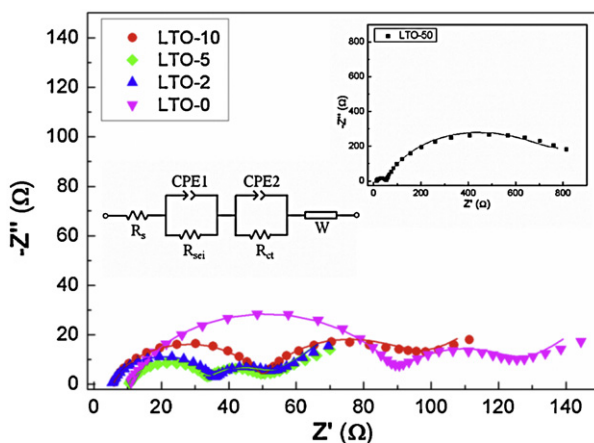


Fig. 8. Nyquist plots of LTO-0, LTO-2, LTO-5, LTO-10 and LTO 50 (solid symbols and solid lines represent experimental and simulated data respectively, and the equivalent circuit is shown in the inset).

placed to represent the double layer capacitance and passivation film capacitance [18]. The values of R_s , R_{sei} and R_{ct} are obtained from the simulated data of EIS in Fig. 8, and listed in Table 2. In Table 2, it can be seen that the R_{sei} of LTO-2, LTO-5, LTO-10 and LTO-50 are obviously lower than that of LTO-0, implying thinner SEI film formed on the former ones than the latter one [28]. One can also see that the R_{ct} of LTO-0 ($32.35\ \Omega$) is higher than that of LTO-2 ($14.77\ \Omega$) and LTO-5 ($16.94\ \Omega$), but lower than that of LTO-10 ($44.25\ \Omega$) and LTO-50 ($657.80\ \Omega$), indicating that only ZrO_2 coating with appropriate thickness (no more than 5 ALD cycles) can increase the charge-transfer reaction at the interface of electrolyte and electrode. Combining EIS with electrochemical performance results, it can be found that LTO electrodes with lower R_{sei} and R_{ct} values (LTO-2 and LTO-5) exhibit better LIB performance than those with higher R_{sei} or/and R_{ct} (LTO-0, LTO-10 and LTO-50). Furthermore, it should be noted that LTO-2, LTO-5 and LTO-10 exhibit lower R_s value than LTO-0 does, suggesting the decreased overall internal resistance with less than 10-cycle ZrO_2 coatings. This also partially accounts for the enhanced LIB performance of LTO-2 and LTO-5. The reason is attributable to improved mechanical adhesion of electrode materials to the current collectors by appropriate ZrO_2 coatings [38].

For the interpretation of the impedance response measured with LTO electrodes, no general consensus has yet been reached, and the results and explanations vary in literatures. For example, Ahn and Xiao [29] claimed that Al_2O_3 coating on LTO electrode could act a barrier restraining the SEI formation, thereby improving the cycling stability and coulombic efficiency of LTO electrode. In another study, carbon coating was found being able to improve the LIB performance of LTO electrode, by promoting formation of thick and successive SEI film on its surface [28]. In the following part, we will try to explain the effect of ZrO_2 coating on the LIB performance of LTO electrode based on the EIS results and electrochemical reaction:



Table 2
Values of the R_s , R_{sei} and R_{ct} obtained by simulated data in Fig. 8.

Resistance sample	R_s (Ω)	R_{sei} (Ω)	R_{ct} (Ω)
LTO-0	10.64	79.43	32.35
LTO-2	5.21	30.57	14.77
LTO-5	10.38	23.16	16.94
LTO-10	5.66	41.84	44.25
LTO-50	11.45	38.64	657.8

The Li-ion insertion into $Li_4Ti_5O_{12}$ consists of three processes: (1) the solvated Li ions diffuse from electrolyte solution to the surface of $Li_4Ti_5O_{12}$; (2) a charge-transfer reaction occurs at the interface between $Li_4Ti_5O_{12}$ and the electrolyte, accompanied by accepting electrons coming from current collector and Li ions from the electrolyte; (3) Li ions diffuse into the bulk $Li_4Ti_5O_{12}$ [9]. Obviously, ZrO_2 coating could mainly affects the charge transfer reaction happened at the interface between $Li_4Ti_5O_{12}$ and the electrolyte, and the working mechanism could be explained by the influence of ZrO_2 coating on the transport of electrons or/and Li ions. (1) On the Li-ion transport. On one hand, EIS result indicates that ZrO_2 coating could effectively accelerate the diffusion of Li ions through SEI film, by reducing the SEI resistance (Table 2). The reason is most likely due to the fact that ZrO_2 coating could prevent the direct contact between LTO and electrolyte, and cover the catalytic sites on the LTO surface for the decomposition of electrolyte, thereby restraining SEI formation and reducing SEI resistance. On the other hand, the artificial ZrO_2 coating layer could also hinder the diffusion of Li ions, because it is not Li-ion conductive. Thus, ZrO_2 coating is a double-sided sword for Li-ion diffusion. The thickness of ZrO_2 coating becomes critically important: it has to be thick enough to reduce SEI resistance, while also has to thin enough to avoid blocking Li-ion diffusion through it. Our study indicates that ZrO_2 coating with no more than 5 ALD cycles is the optimized parameter. (2) On the electron transport. Previous studies have shown that direct metal oxide coating on electrode could not only maintain the electron pathways between active materials and carbon additives [35], but also improve the adhesion of electrode materials to the current collector [38], thereby improving the electron transport among them. In our case, therefore, it can be considered that direct ZrO_2 coating on LTO electrode acts as the similar way to improve electron transport (as disclosed by the reduced R_s in Table 2) and contribute to the reduced charge-transfer resistance of LTO-2 and LTO-5 compared with that of LTO-0 (Table 2). It is worthy to mention that the increased charge-transfer resistance of LTO-10 and LTO-50 results from the blocked Li-ion diffusion due to thicker ZrO_2 coating with low electronic conductivity. In those cases, the improvement from electron transport becomes neglected.

In summary, ZrO_2 coating with less than 10 ALD cycles can enhance the specific capacity, cycling performance and rate capability of the LTO between 0.1 and 2.5 V. The reason could be attributed to the suppressed SEI formation and the improved electron transport by coating ultrathin ZrO_2 film directly on the LTO electrode. ZrO_2 coating with more than 10 ALD cycles would worsen the electrochemical performance of the LTO, probably due to the blocking effect of thick ZrO_2 coating on the lithium ion diffusion. Moreover, ZrO_2 coating can decrease the specific capacity of the LTO by adding extra weight to the electrode materials, without contributing any capacity to lithium ion storage. This situation becomes more and more non-negligible with increasing ALD cycles. As a result, LTO-50 has obvious higher weight of the electrode materials than the others due to the thick ZrO_2 coating. Therefore, the additional weight of ZrO_2 coating is another reason for the lowered specific capacity of LTO-50 than LTO-0 (Fig. 7).

4. Conclusions

ZrO_2 coating was conducted directly on the $Li_4Ti_5O_{12}$ electrode by atomic layer deposition with different cycles (0, 1, 2, 5, 10 and 50). The results indicated that ZrO_2 coating with less than 10 ALD cycles could enhance the specific capacity, cycling stability and rate capability of the $Li_4Ti_5O_{12}$ electrode in a voltage range of 0.1–2.5 V. The mechanism study by EIS revealed that the reason for the enhanced LIB performance was mainly due to the suppressed SEI formation and the improved electron transport by ultrathin

ZrO₂ coating. This work provides a novel and effective approach to improve the electrochemical performance of anode materials via surface-modification by atomic layer deposition. It is believed that this work will be inspirable for other researchers and beneficial for the development of lithium ion batteries used in PHEVs and EVs.

Acknowledgements

This research was supported by General Motors of Canada, Natural Sciences and Engineering Research Council of Canada (NSERC), Canada Research Chair (CRC) Program, Canada Foundation for Innovation (CFI), Ontario Research Fund (ORF), Ontario Early Researcher Award (ERA) and University of Western Ontario.

Appendix A. Supplementary data

Supplementary data associated with this article can be found, in the online version, at <http://dx.doi.org/10.1016/j.electacta.2012.12.141>.

References

- [1] M. Armand, J.-M. Tarascon, Building better batteries, *Nature* 451 (2008) 652.
- [2] J.-M. Tarascon, Key challenges in future Li-battery research, *Philosophical Transactions of the Royal Society A* 368 (2010) 3227.
- [3] N.A. Kaskhedikar, J. Maier, The effect of the charging protocol on the cycle life of a Li-ion battery, *Advanced Materials* 21 (2009) 2664.
- [4] E. Ferg, R.J. Gummow, A. de Kock, M.M. Thackeray, Spinel anodes for lithium-ion batteries, *Journal of the Electrochemical Society* 141 (1994) L147.
- [5] P. Liu, E. Sherman, M. Verbrugge, Electrochemical and structural characterization of lithium titanate electrodes, *Journal of Solid State Electrochemistry* 14 (2010) 585.
- [6] C.Y. Ouyang, Z.Y. Zhong, M.S. Lei, Ab initio studies of structural and electronic properties of Li₄Ti₅O₁₂ spinel, *Electrochemistry Communications* 9 (2007) 1107.
- [7] T.-F. Yi, Y. Xie, Y.-R. Zhu, R.-S. Zhu, H. Shen, Structural and thermodynamic stability of Li₄Ti₅O₁₂ anode material for lithium-ion batteries, *Journal of Power Sources* 222 (2013) 448.
- [8] C.H. Chen, J.T. Vaughey, A.N. Jansen, D.W. Dees, A.J. Kahaian, T. Goacher, M.M. Thackeray, Studies of Mg-substituted Li_{4-x}Mg_xTi₅O₁₂ spinel electrodes ($0 \leq x \leq 1$) for lithium batteries, *Journal of the Electrochemical Society* 148 (2001) A102.
- [9] G.N. Zhu, Y.G. Wang, Y.Y. Xia, Ti-based compounds as anode materials for Li-ion batteries, *Energy & Environmental Science* 5 (2012) 6652.
- [10] T.F. Yi, L.J. Jiang, J. Shu, C.B. Yue, R.S. Zhu, H.B. Qiao, Recent development and application of Li₄Ti₅O₁₂ as anode material of lithium ion battery, *Journal of Physics and Chemistry of Solids* 71 (2010) 1236.
- [11] J. Li, Z. Tang, Z. Zhang, Controllable formation and electrochemical properties of one-dimensional nanostructured spinel Li₄Ti₅O₁₂, *Electrochemistry Communications* 7 (2005) 894.
- [12] C. Lai, Y.Y. Dou, X. Li, X.P. Gao, Improvement of the high rate capability of hierarchical structured Li₄Ti₅O₁₂ induced by the pseudocapacitive effect, *Journal of Power Sources* 195 (2010) 3676.
- [13] E.M. Sorensen, S.J. Barry, H.K. Jung, J.M. Rondinelli, J.T. Vaughey, K.R. Poepelmeier, Three-dimensionally ordered macroporous Li₄Ti₅O₁₂: effect of wall structure on electrochemical properties, *Chemistry of Materials* 18 (2006) 482.
- [14] J. Haetge, P. Hartmann, K. Brezesinski, J. Janek, T. Brezesinski, Ordered large-pore mesoporous Li₄Ti₅O₁₂ spinel thin film electrodes with nanocrystalline framework for high rate rechargeable lithium batteries: relationships among charge storage, electrical conductivity, and nanoscale structure, *Chemistry of Materials* 23 (2011) 4384.
- [15] L. Cheng, J. Yan, G.N. Zhu, J.Y. Luo, C.X. Wang, Y.Y. Xia, General synthesis of carbon-coated nanostructure Li₄Ti₅O₁₂ as a high rate electrode material for Li-ion intercalation, *Journal of Materials Chemistry* 20 (2010) 595.
- [16] L. Zhao, Y.S. Hu, H. Li, Z. Wang, L. Chen, Porous Li₄Ti₅O₁₂ coated with N-doped carbon from ionic liquids for Li-ion batteries, *Advanced Materials* 23 (2011) 1385.
- [17] S. Huang, Z. Wen, X. Zhu, Z. Gu, Preparation and electrochemical performance of Ag doped Li₄Ti₅O₁₂, *Electrochemistry Communications* 6 (2004) 1093.
- [18] L. Shen, C. Yuan, H. Luo, X. Zhang, K. Xu, F. Zhang, In situ growth of Li₄Ti₅O₁₂ on multi-walled carbon nanotubes: novel coaxial nanocables for high rate lithium ion batteries, *Journal of Materials Chemistry* 21 (2011) 761.
- [19] H.G. Jung, M.W. Jang, J. Hassoun, Y.K. Sun, B. Scrosati, A high-rate long-life Li₄Ti₅O₁₂/Li[Ni_{0.45}Co_{0.1}Mn_{1.45}]O₄ lithium-ion battery, *Nature Communications* 2 (2011) 516.
- [20] T.F. Yi, Y. Xie, J. Shu, Z. Wang, C.B. Yue, R.S. Zhu, H.B. Qiao, Structure and electrochemical performance of Niobium-substituted spinel lithium titanium oxide synthesized by solid-state method, *Journal of the Electrochemical Society* 158 (2011) A266.
- [21] J. Shu, Study of the interface between Li₄Ti₅O₁₂ electrodes and standard electrolyte solutions in 0.0–5.0 V, *Electrochemical and Solid-State Letters* 11 (2008) A238.
- [22] H. Ge, N. Li, D. Li, C. Dai, D. Wang, Electrochemical characteristics of spinel Li₄Ti₅O₁₂ discharge to 0.01 V, *Electrochemistry Communications* 10 (2008) 719.
- [23] X.L. Yao, S. Xie, H.Q. Nian, C.H. Chen, Spinel Li₄Ti₅O₁₂ as a reversible anode material down to 0 V, *Journal of Alloys and Compounds* 465 (2008) 375.
- [24] T.F. Yi, J. Shu, Y.R. Zhu, X.D. Zhu, C.B. Yue, A.N. Zhou, R.S. Zhu, High-performance Li₄Ti_{5-x}V_xO₁₂ ($0 \leq x \leq 0.3$) as an anode materials for secondary lithium-ion batteries, *Electrochimica Acta* 54 (2009) 7464.
- [25] T.F. Yi, Y. Xie, L.J. Jiang, J. Shu, C.B. Yue, A.N. Zhou, M.F. Ye, Advanced electrochemical properties of Mo-doped Li₄Ti₅O₁₂ anode material for power lithium ion battery, *RSC Advances* 2 (2012) 3541.
- [26] T.F. Yi, J. Shu, Y.R. Zhu, X.D. Zhu, R.S. Zhu, A.N. Zhou, Advanced electrochemical performance of Li₄Ti_{4.95}V_{0.05}O₁₂ as a reversible anode material down to 0 V, *Journal of Power Sources* 195 (2010) 285.
- [27] W. Lu, I. Belharouak, J. Liu, K. Amine, Electrochemical and thermal investigation of Li_{4/3}Ti_{5/3}O₄ spinel, *Journal of the Electrochemical Society* 154 (2007) A114.
- [28] Y.B. Ye, F. Ning, B. Li, Q.S. Song, W. Lv, H. Du, D. Zhai, F. Su, Q.H. Yang, F. Kang, Carbon coating to suppress the reduction decomposition of electrolyte on the Li₄Ti₅O₁₂ electrode, *Journal of Power Sources* 202 (2012) 253.
- [29] D. Ahn, X. Xiao, Extended lithium titanate cycling potential window with near zero capacity loss, *Electrochemistry Communications* 13 (2011) 796.
- [30] X. Meng, X.Q. Yang, X. Sun, Emerging applications of atomic layer deposition for lithium-ion battery, *Advanced Materials* 24 (2012) 3589.
- [31] H.C.M. Knoops, M.E. Donders, M.C.M. van de Sanden, P.H.L. Notten, W.M.M. Kessels, Atomic layer deposition for nanostructured Li-ion batteries, *Journal of Vacuum Science and Technology A* 30 (2012) 010801.
- [32] S.M. George, Atomic layer deposition, *Chemical Reviews* 110 (2010) 111.
- [33] X. Xiao, P. Lu, D. Ahn, Ultrathin multifunctional oxide coatings for lithium ion batteries, *Advanced Materials* 23 (2011) 3911.
- [34] Y. He, X. Yu, Y. Wang, H. Li, X. Huang, Alumina-coated patterned amorphous silicon as the anode for a lithium-ion battery with high coulombic efficiency, *Advanced Materials* 43 (2011) 4938.
- [35] Y.S. Jung, A.S. Cavanagh, L.A. Riley, S.-H. Kang, A.C. Dillon, M.D. Groner, S.M. George, S.-H. Lee, Ultrathin direct atomic layer deposition on composite electrodes for highly durable and safe Li-ion batteries, *Advanced Materials* 22 (2010) 2172.
- [36] E. Kang, Y.S. Jung, A.S. Cavanagh, G.-H. Kim, S.M. George, A.C. Dillon, J.K. Kim, J. Lee, Fe₃O₄ nanoparticles confined in mesocellular carbon foam for high performance anode materials for lithium-ion batteries, *Advanced Functional Materials* 21 (2011) 2430.
- [37] L.A. Riley, A.S. Cavanagh, S.M. Geroge, Y.S. Jung, Y. Yan, S.H. Lee, A.C. Dillon, Conformal surface coatings to enhance high volume expansion Li-ion anode materials, *ChemPhysChem* 11 (2010) 2124.
- [38] L.A. Riley, A.S. Cavanagh, S.M. Geroge, S.-H. Lee, A.C. Dillon, Improved mechanical integrity of ALD-coated composite electrodes for Li-ion batteries, *Electrochemical and Solid-State Letters* 14 (2011) A29.
- [39] I.R.M. Kottekoda, Y. Kadoma, H. Ikuta, Y. Uchimoto, M. Wakihara, Enhancement of rate capability in graphite anode by surface modification with zirconia, *Electrochemical and Solid-State Letters* 5 (2002) A275.
- [40] J. Cho, Y.S. Kim, T.J. Kim, B. Park, Zero-strain intercalation cathode for rechargeable Li-ion cell, *Angewandte Chemie International Edition* 40 (2001) 3367.
- [41] C. Li, H.P. Zhang, L.J. Fu, H. Liu, Y.P. Wu, E. Rahm, R. Holze, H.Q. Wu, Cathode materials modified by surface coating for lithium ion batteries, *Electrochimica Acta* 51 (2006) 3872.
- [42] J. Liu, X. Li, J. Yang, D. Geng, Y. Li, D. Wang, R. Li, X. Sun, M. Cai, M.W. Verbrugge, Microwave-assisted hydrothermal synthesis of nanostructured spinel Li₄Ti₅O₁₂ as anode materials for lithium ion batteries, *Electrochimica Acta* 6 (2012) 100.
- [43] J. Liu, X. Meng, M.N. Banis, M. Cai, R. Li, X. Sun, Crystallinity-controlled synthesis of zirconium oxide thin films on nitrogen-doped carbon nanotubes by atomic layer deposition, *Journal of Physical Chemistry C* 116 (2012) 14656.
- [44] D.M. Hausmann, E. Kim, J. Becker, R.G. Gordon, Atomic layer deposition of hafnium and zirconium oxides using metal amide precursors, *Chemistry of Materials* 14 (2002) 4350.
- [45] H. Ge, N. Li, D. Li, C. Dai, D. Wang, Study on the theoretical capacity of spinel lithium titanate induced by low-potential intercalation, *Journal of Physical Chemistry C* 113 (2009) 6324.